Research article

Polyvinyl alcohol increased growth, migration, invasion, and sphere size in the PK-8 pancreatic ductal adenocarcinoma cell line

Fujiya Gomi [a,1], Norihiko Sasaki [b,1], Yuuki Shichi [a], Fuuka Minami [c], Seiichi Shinji [a,d], Masashi Toyoda [b], Toshiyuki Ishiwata [a,*]

[a] Division of Aging and Carcinogenesis, Research Team for Geriatric Pathology, Tokyo Metropolitan Institute of Gerontology, Tokyo 173-0015, Japan
[b] Research Team for Geriatric Medicine (Vascular Medicine), Tokyo Metropolitan Institute of Gerontology, Tokyo 173-0015, Japan
[c] Department of Veterinary Pathology, School of Veterinary Medicine, Nippon Veterinary and Life Science University, Tokyo 180-8602, Japan
[d] Departments of Gastrointestinal and Hepato-Biliary-Pancreatic Surgery, Nippon Medical School, Tokyo 113-8603, Japan

ARTICLE INFO

ABSTRACT

Polyvinyl alcohol (PVA) is a water-soluble synthetic polymer used in eye drops, embolization particles, and artificial cartilage. It has also been shown to cause expansion of functional multipotent self-renewing hemato-poietic stem cells under serum-free conditions. In this study, we examined the effects of PVA on human pancreatic ductal adenocarcinoma (PDAC) cell lines using 2-dimensional (2D) and 3D-cultures with serum-free medium. In the 2D-culture, PVA-treatment induced an aggregated colony-like appearance in PDAC cells. It increased the growth of PK-8 cells in a dose-dependent manner as well as significantly increasing migration and invasion abilities. qRT-PCR showed an increase in α2 integrin and a decrease in matrix metalloprotease levels in PVA-treated PK-8 cells. Through qRT-PCR analysis, β1 integrin expression at the mRNA level was found to be decreased; however, it was unaltered at the protein level when assessed using FACS analysis.

PVA further induced mesenchymal to epithelial transition-like alterations, including increased E-cadherin and decreased Vimentin and N-cadherin expression. Four cancer stem cell (CSC) markers were higher in PVA-treated PK-8 cells compared to controls. In 3D-culture, PVA-treated PK-8 cells showed a rod-like appearance with larger sphere size and higher growth ability. qRT-PCR showed that CSC markers did not increase and 2 of 4 drug transporters had decreased in PVA-treated PK-8 cells. These findings suggest that PVA increases the growth, migration, invasion, and sphere size of PK-8 cells, but does not increase the proportion of pancreatic CSCs under 3D-culture conditions with serum-free medium.

1. Introduction

Pancreatic cancer is one of the most lethal malignant tumors, with 5-year overall survival rates below 9% [1]. Pancreatic ductal adenocarcinoma (PDAC) is the most common subtype of pancreatic cancer, accounting for approximately 90% of all pancreatic malignancies [2]. By 2030, pancreatic cancer is projected to be the second leading cause of cancer-related death in the United States [3]. Surgery offers the only possible cure; however, 80% of patients with PDAC have tumors that are inoperable at diagnosis. Even patients who do undergo surgery experience a high incidence of post-operative tumor recurrence and metastasis. With a rapidly aging population, an increase in pancreatic cancer-related deaths is expected worldwide.

Recent studies have shown that PDAC consists of a heterogeneous population of cancer cells, which includes a small number of cells called cancer stem cells (CSCs) [4, 5, 6]. A CSC is defined as "a cell within a tumor that possesses the capacity to self-renew and to generate heterogeneous lineages of cancer cells that comprise the tumor" [7]. Based on the concept that CSCs are solely responsible for tumor self-renewal, it has been suggested that elimination of CSCs could lead to a curative treatment for PDAC.

Concentrated or aggregated CSCs are important experimental targets to determine the characteristics of CSCs and to develop novel anti-CSC therapies. In the sphere-formation assay, cancer cells cultured in ultra-low attachment plates are commonly used to enrich the potential CSC subpopulations [5]. Sphere-formation assays of PDAC cells were

---

originally cultured in serum-free medium containing epidermal growth factor (EGF) and fibroblast growth factor (FGF)-2, following the neurosphere formation method. However, under these culture conditions the majority of the PDAC cells were not able to expand greatly in number or to form large spheres. Recently, we reported that PDAC cells form larger spheres and have higher levels of CSC marker expression in medium containing 10% fetal bovine serum (FBS) than in the presence of EGF and FGF-2 [8]. However, a concern with this method is that differences between lots of fetal bovine serum may affect the experimental results. Serum albumin has also been recognized as a major source of biological contaminants in hematopoietic cell cultures.

Polyvinyl alcohol (PVA) is a water-soluble synthetic polymer used in glue, papermaking, textiles, and a variety of coatings. It has also been used in medical applications, including soft contact lenses, eye drops, embolization particles, tissue adhesion barriers, and artificial cartilage [9]. Recently, an albumin-free culture system that supports the long-term ex-vivo expansion of functional mouse hematopoietic stem cells (HSCs) was reported [10]. PVA was found to induce marked expansion of functional multipotent self-renewing HSCs under serum-free conditions. PVA was therefore identified as a functionally superior replacement for serum albumin that is compatible with good manufacturing practices.

In the present study, we examined the biological effects of PVA on PDAC cells in 2D-culture. Furthermore, we clarified whether PVA with serum-free medium containing growth factors induces formation of PDAC spheres with a high proportion of CSCs.

2. Materials and methods

2.1. Cell culture

Human PDAC cell lines PK-1 and MIA PaCa-2 were obtained from the Cell Resource Center for Biomedical Research, Institute of Development, Aging, and Cancer, Tohoku University (Sendai, Japan). Human PDAC PK-8 cells were provided by the RIKEN BRC through the National Bio-Resource Project of the MEXT, Japan. In the 2D-culture, PDAC cells were cultured in growth medium including RPMI 1640 medium supplemented with FGF-2 (10 ng/mL, ReproCELL, Tokyo, Japan) and EGF (20 ng/mL, AUSTRAL Biologicals, San Ramon, CA, USA) at 37 °C with 5% CO_2. In the PVA-treated group, PVA (363081, Sigma-Aldrich, St. Louis, MO, USA) was added to the cell cultures at the indicated concentrations for 7 days. The cells were photographed using a phase contrast microscope (CK-40, Olympus).

2.2. Morphology and measurement of the sphere area

To form spheres, cells (1.0×10^3 cells/well) were cultured in 24-well ultra-low attachment plates (Corning Inc. Kennebunk, ME, USA) with RPMI 1640 medium containing FGF-2 and EGF for 7 days. PVA was added at the beginning of the culture period at 0.1% (final concentration). Photography and evaluation of the spheres (4 samples per group) were performed using a Cell3iMager Duos sphere-analyzing system (SCREEN Holdings Co. Ltd., Kyoto, Japan).

2.3. Scanning electron microscopy (SEM)

Adherent PDAC cells were fixed with 2.5% glutaraldehyde in a 0.1 M phosphate buffer for 30 min at 4 °C followed by 1% OsO_4 for 30 min at 4 °C. PK-8 cell spheres were collected and fixed with 2.5% glutaraldehyde in a 0.1 M phosphate buffer for 2 h at 4 °C followed by 1% OsO_4 dissolved in distilled water for 30 min at 4 °C. After dehydration via a graded ethanol series, the cells were coated with a platinum layer using an MSP-1S sputter coater (Shinku Device, Ibaraki, Japan), and photographed using a Phenom Pro desktop scanning electron microscope (Thermo Fisher Scientific Inc., Waltham, MA, USA).

2.4. Confocal laser microscopy

PK-8 cells were cultured for 7 days in 24-well ultra-low attachment plates in RPMI 1640 medium supplemented with FGF-2 and EGF. PVA was added at the beginning of the culture period to 0.1% final concentration. Spheres were fixed in 4% paraformaldehyde solution for 1 h at 4 °C. The spheres were incubated with anti-human E-cadherin monoclonal antibodies (clone HECD-1, 1:200 dilution; Takara Bio Inc., Shiga, Japan) for 1 h at room temperature (RT), followed by Alexa 488-labeled anti-mouse IgG antibodies (1:500 dilution; Cell Signaling Technology, Danvers, MA, USA) for 1 h at RT. Nuclear staining was performed using 4′,6-diamidine-2′-phenylindole dihydrochloride (DAPI) for 30 min at RT. The maximum intensity projection (MIP) and slice view images were obtained using an inverted confocal microscope equipped with regular objectives (S Plan Fluor ELWD, 20x) using a Nikon Eclipse Ti2 with an A1RHD25 laser-scanning confocal head equipped with two different lasers (excitation at 405 and 488 nm) (Nikon Solutions Co., Ltd., Tokyo, Japan).

2.5. Cell proliferation assays

The WST-8 assay was performed for 2D-cultures, and the ATP assay was employed for sphere cell proliferation assays, as previously described [11, 12]. In the WST-8 assay, PK-8 cells were cultured in growth medium at a density of 5.6×10^3 cells/well in 96-well plates and incubated for 7 days. Adherent cells were then incubated with WST-8 cell counting reagent (Wako Pure Chemical Industries, Osaka, Japan) for 2 h. The optical density was measured at 450 nm using a plate reader (Bio-Rad Laboratories, Hercules, CA). For the ATP assay, cells were cultured in growth medium at a density of 3×10^3 cells/well in 96-well ultra-low attachment plates (Thermo Fisher Scientific, Waltham, MA, USA) and incubated for 7 days. ATP assays were used to examine proliferation using the CellTiter-Glo® 2.0 Assay (Promega, Madison, USA), according to the manufacturer's protocol. These experiments were performed in triplicate.

2.6. Migration and invasion assays

A cell migration assay was carried out using the Boyden chamber technique, as previously reported [12]. Cell culture inserts with 8-µm pore size and 6.4 mm diameter (Corning Inc., Corning, NY, USA) were used according to the manufacturer's instructions. Briefly, cells were suspended in 500 µL of serum-free medium and placed onto the upper component of the inserts at a density of 1×10^5 cells/well. The lower compartment was filled with 750 µL medium containing 10% FBS, and the cells were incubated at 37 °C in a 5% CO_2 atmosphere. After 8 h, the cells on the upper surface of the membrane were carefully removed with a cotton swab. Cells that had migrated through the membrane to the lower surface of the filter were fixed and stained with a Diff-Quick staining kit (Polysciences Inc., Warrington, PA, USA) and counted under a light microscope. Invasion assays were performed using Matrigel-coated cell culture inserts with 8-µm pore size and 6.4 mm in diameter (Discovery Labware Inc., Bedford, MA, USA) as previously reported [13]. The cells were suspended in 500 µL of serum-free medium and placed onto the upper component of the inserts at a density of 1×10^5 cells/well. The lower compartment was filled with 750 µL of medium containing 10% FBS. After 16 h, the cells on the upper surface of the membrane were carefully removed with a cotton swab. Cells that had migrated through the membrane to the lower surface of the filter were fixed and stained with a Diff-Quick and counted under a light microscope. These experiments were performed in duplicate.

2.7. Quantitative reverse transcription polymerase chain reaction (qRT-PCR)

PK-8 cells were cultured with growth medium with or without PVA (final concentration: 0.1%) for 7 days at a concentration of 1.0×10^3

cells/well for 2D-culture or 3×10^3 cells/well in 96-well ultra-low attachment plates for 3D-culture. Total RNA was isolated from cells using an RNeasy Plus Mini Kit (QIAGEN, Hilden, Germany) and was subsequently reverse-transcribed using the ReverTra Ace® qPCR RT Kit (Toyobo, Osaka, Japan). qRT-PCR was performed using the Power Sybr® Green kit (Applied Biosystems, Foster City, CA, USA) and the StepOne-Plus™ real-time PCR system (Applied Biosystems). ß-Actin was amplified and used as an internal control. The threshold value was noted for each transcript and normalized to the internal control. The relative quantitation of each mRNA was performed using the comparative Ct method. Primer sets for qRT-PCR are listed in Supplemental Table 1. Gene expression measurements were performed in duplicate.

2.8. Fluorescence activated cell sorter (FACS) analysis

FACS analysis was performed as described previously [13]. The following primary antibodies were used: anti-CD44v9 (Cosmo Bio Co., Ltd., Japan), anti-CD24 (Santa Cruz Biotechnology, Dallas, TX, USA), anti-α2-integrin (Merck Millipore, Billerica, MA, USA), and anti-β1-integrin (Abcam, Cambridge, UK). Mean fluorescence intensity (MFI) was calculated by subtracting the intensities of the control samples. These experiments were independently performed three times.

2.9. Immunoblotting

Cellular protein was isolated using lysis buffer (50 mM Tris-HCl pH 7.4, 150 mM NaCl, and 1% [v/v] Triton™ X-100) containing protease- and phosphatase-inhibitor cocktails (Roche, Indianapolis, IN, USA). Protein lysates were separated by SDS-PAGE on an 8% gel and then transferred onto PVDF membranes (Merck Millipore). After blocking, the membranes were incubated with the following primary antibodies: polyclonal rabbit anti-Nanog (ReproCELL), monoclonal mouse anti-Sox2 (Merck Millipore), or monoclonal mouse anti-β-actin (Sigma-Aldrich). The membranes were then incubated with the appropriate peroxidase-conjugated secondary antibodies (Cell Signaling Technology), washed, and developed with ECL™ Prime reagents (GE Healthcare, Piscataway, NJ, USA). Two independent experiments were performed.

2.10. Statistical analysis

Quantitative data are presented as mean ± standard deviation (SD). Statistical analysis was performed using EZR (Saitama Medical Centre, Jichi Medical University; http://www.jichi.ac.jp/saitama-sct/SaitamaHP.files/statmedEN.html; Kanda, 2012). Unpaired Student's t-test and one-way ANOVA with Tukey's HSD test were used to compare two or more groups, respectively. A value of $p < 0.05$ was considered statistically significant.
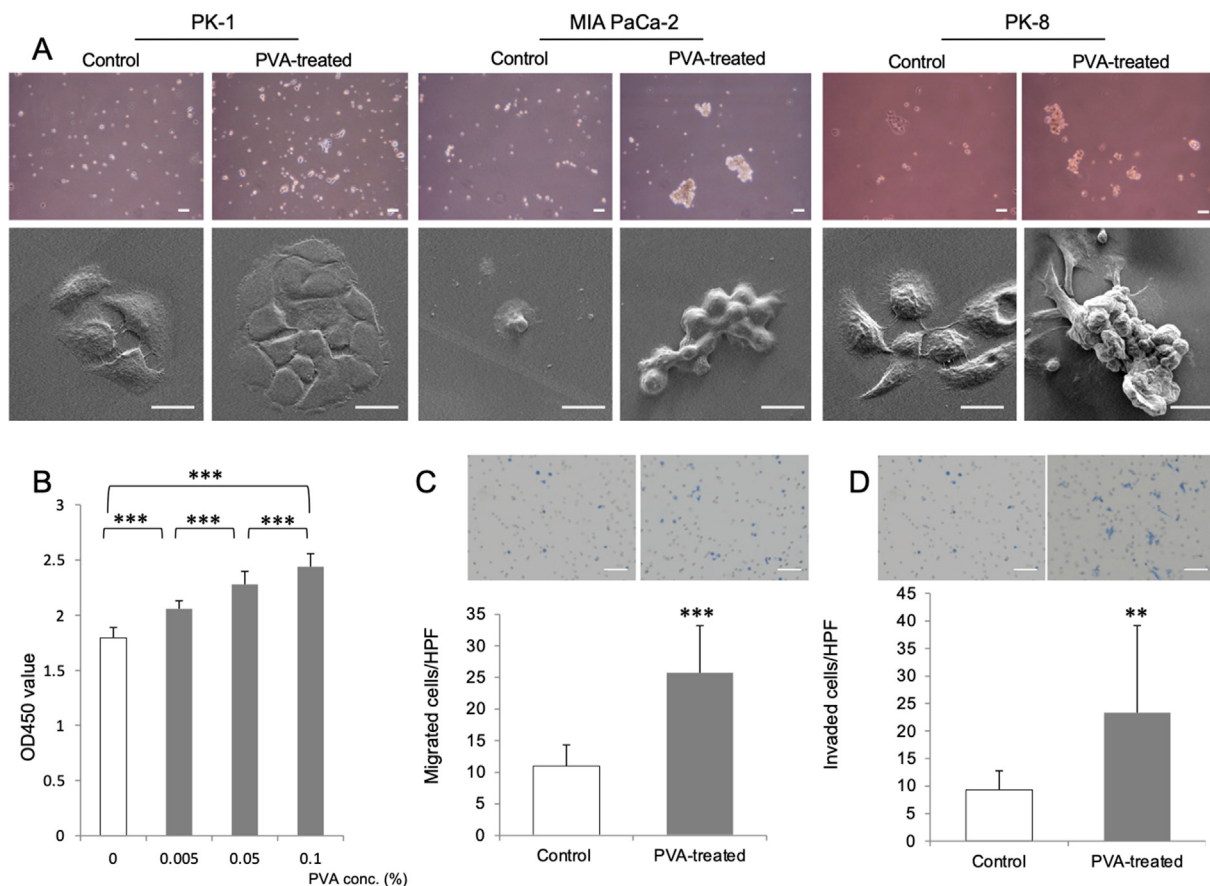

Figure 1. Morphology, growth, migration, and invasion of PVA-treated PDAC cells under 2D-culture conditions. (A) Representative phase contrast and SEM images of PVA-treated PDAC cells under adherent culture conditions. Scale bar in the phase contrast images: 100 μm, SEM images: 20 μm. (B) WST-8 assay of PVA-treated PK-8 cells. (C) Cell migration assay of PVA-treated PK-8 cells. (D) Cell invasion assay of PVA-treated PK-8 cells. Scale bar in the migration and invasion assays: 100 μm. **p < 0.01, ***p < 0.001.

3. Results

3.1. Morphological analyses of PVA-treated PDAC cells in 2D-culture

Under the 2D-culture conditions, PVA-treated PDAC cells, including PK-1, MIA PaCa-2, and PK-8 cells, showed an aggregated colony-like appearance under phase-contrast microscopy (Figure 1A, upper panels). SEM analysis of the PVA-treated group showed a flat alveolar structure in the PK-1 cells, and raised mountain-like colonies in the MIA PaCa-2 and PK-8 cells (Figure 1A, lower panels). PK-8 formed larger and taller colonies than the MIA PaCa-2 cells after PVA administration. Follow-up experiments focused on the PK-8 cells that showed the most characteristic morphological alterations after the addition of PVA.

3.2. Biological behaviors of PVA-treated PK-8 cells under 2D-culture

The increase of PVA from 0.005% to 0.1% significantly increased the growth of PK-8 cells in a dose-dependent manner (Figure 1B). Furthermore, PVA-treated cells demonstrated a >2-fold higher migration through 8-μm pores or invasion through Matrigel-coated membranes with 8-μm pores compared to the non-treated control cells (Figure. 1C and D, respectively).

3.3. Expression of adhesion molecules, CSC markers, and epithelial to mesenchymal transition markers in PVA-treated PK-8 cells under 2D-culture

To examine the mechanism underlying the increased migration and invasion of PVA-treated PK-8 cells, we compared the levels of various integrin subunits in PVA-treated and control PK-8 cells by qRT-PCR. We found that in PVA-treated cells, the mRNA level of the β1 integrin subunit was significantly lower, while that of the α2 integrin subunit was significantly higher, compared to that in control cells (Figure 2A, upper panel). FACS analysis showed a significant increase in the expression of the α2 integrin subunit; however, the expression of the β1 integrin subunit was unaltered at the protein level (Figure 2B). One of the key features of invasion is increased production of matrix metalloproteinases (MMPs), including MMP2, MMP9, and MT1-MMP. PVA-treated cells showed significantly higher invasive capacity, but MT1-MMP, MMP2, and MMP9 mRNA was lower than in the control cells. Since EMT is one of the earliest steps in the metastasis of cancer cells, we examined the mRNA expression levels of EMT markers. The mRNA expression levels of *E-cadherin* and *Snail* were significantly higher in PVA-treated PK-8 cells. In contrast, PVA-treated cells expressed lower levels of *Vimentin, N-cadherin*, and *Slug* (Figure 2C, upper panel). These expression patterns are similar to the mesenchymal to epithelial transition (MET) of the cells. Next, we compared the mRNA expression levels of several pancreatic CSC markers. PVA-treated PK-8 cells expressed higher levels of 4 of the 7 CSC markers that we assessed, including *Oct3/4, Nanog, Sox2*, and *ALDH1*, but *Nestin* expression was significantly lower in PVA-treated cells than in control cells (Figure 2D, upper panel). Western blot analyses showed that PVA-treated PK-8 cells expressed higher protein levels of Nanog and Sox2 compared to untreated control cells (Figure 2E). CD24 expression was lower in PVA-treated PK-8 cells, while CD44v9 expression was not altered after PVA treatment (Figure 2F). MIA PaCa-2 cells that formed smaller and lower-height colonies after PVA treatment showed increased *Snail* and *CD24* mRNA levels by qRT-PCR (Figure. 2A, C, D lower panels).

3.4. Morphological analyses and cell growth ability of PVA-treated PK-8 cells in 3D-culture

Under 3D-culture conditions using ultra-low attachment plates, PK-8 cells formed round to oval-shaped spheres, while PVA-treated cells demonstrated a rod-like appearance (Figure 3A). E-cadherin (green) was localized at the cell membrane of PK-8 cells, and it was expressed at the periphery of spheres from PVA-treated and control PK-8 cells. The area of the spheres was markedly larger in the PVA-treated cells than in the control cells (Figure 3B), and cell growth was also higher in the PVA-treated cells than in the control cells (Figure 3C). These findings indicate that PVA induced cell proliferation and the formation of larger spheres under 3D-culture conditions.

3.5. Expression of CSC markers and drug transporters in PVA-treated spheres

To examine whether the enlarged PVA-treated spheres had a higher proportion of CSCs, we performed qRT-PCR of CSC markers. There were no statistically significant increases in CSC markers in the PVA-treated PK-8 or MIA PaCa-2 spheres compared to the control spheres. Three of the seven CSC markers (*Nanog, Sox2*, and *ALDH1*) were significantly decreased in the PVA-treated PK-8 groups (Figure 4A). Western blotting showed decreased protein levels of Nanog and Sox2 in the PVA-treated PK-8 cells (Figure 4B). FACS analysis showed that expression of the cell surface marker CD24 was decreased, and CD44v9 was not changed, in PVA-treated PK-8 cells (Figure 4C). CSCs are known to be resistant to anti-cancer drugs because of their high expression of drug transporters. No drug transporter was found to be significantly increased in the PVA-treated PK-8 or MIA PaCa-2 spheres. The expression levels of *ABCB1* and *ABCC1* were significantly decreased in the PVA-treated PK-8 spheres, whereas *ABCC2* expression was decreased in the MIA PaCa-2 spheres (Figure 4D). These findings suggest that the proportion of CSCs were not increased in the PVA-induced large spheres.

4. Discussion

Orally administered PVA has been reported to be relatively harmless because it has low acute oral toxicity, is poorly absorbed from the gastrointestinal tract, does not accumulate in the body, and is neither mutagenic nor clastogenic [14]. PVA hydrogels have been used in various biomedical and pharmaceutical applications, including the lining for artificial hearts and drug delivery [15]. A recent study showed that PVA and *p*-boronophenylalanine (BPA) formed complexes and exhibited efficient tumor accumulation and prolonged tumor retention. PVA-BPA demonstrated critically enhanced antitumor activity in boron neutron capture therapy [16]. In pancreatic cancer research, PVA is used as a drug delivery system as well as scaffolding for 3D-culture and anti-cancer drug eluting beads [17, 18, 19]. To our knowledge, there have been no previous studies into the direct effects of PVA on the biological behaviors of PDAC cells *in vitro*. In this study, PVA induced aggregation of the PDAC cells as well as piling up of MIA PaCa-2 and PK-8 cells into mountain-like colonies. This may be due to an increase in cell proliferation, migration, and MET, including increased E-cadherin expression and a decrease in vimentin expression, in PDAC cells. Although PVA increased the invasive capacity of the PK-8 cells compared to the non-treated control cells, MMPs were decreased in PK-8 cells compared to the control cells. The roles of MMPs have previously been studied in PDACs. Several MMPs, including MMP2, MMP7, MMP9, and MMP14 (MT1-MMP), have been reported to contribute to the aggressiveness of the cancer [20, 21]. Thus, there may be additional mechanisms that contribute to the increase in invasive capacity after the addition of PVA to PK-8 cells. After PVA treatment, the mRNA level of β1 integrin was decreased, while the protein level of β1 integrin remained unaltered. Integrins exist as heterodimers, and β1 integrin is the main integrin and is expected to be abundant. Even if the mRNA level of β1 integrin is reduced, it may take time for an appreciable decrease to occur at the protein level. This may be due to its abundance and lifespan. In contrast, α2 integrin, which contribute to cell-matrix adhesiveness mediated by complex with β1 integrin, was increased after the addition of PVA. Further studies are
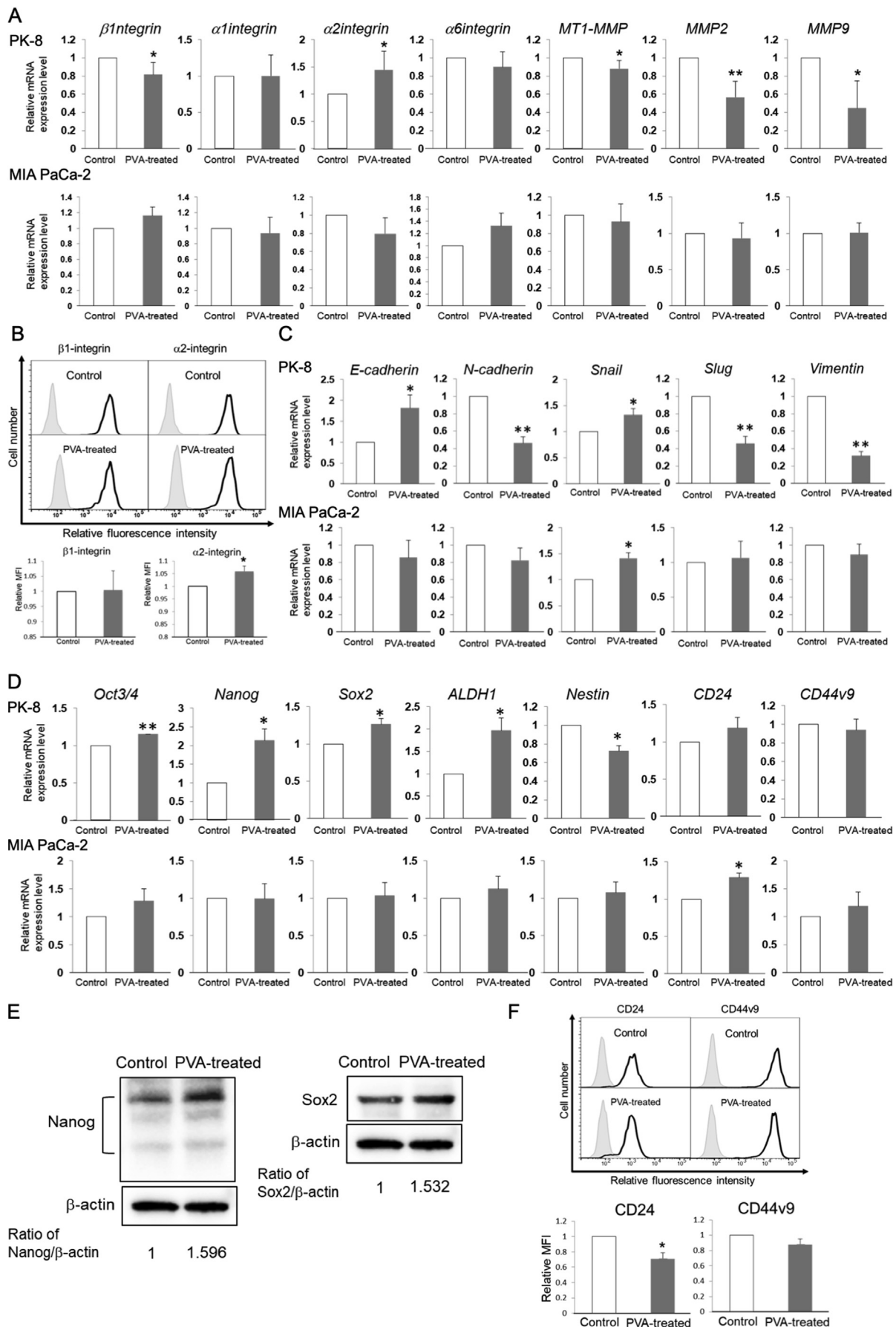
(caption on next page)

Figure 2. Expression of adhesion molecules, EMT markers, and CSC markers in PVA-treated cells under 2D-culture conditions. Comparative expression of (A) adhesion molecules, (C) epithelial-to-mesenchymal transition (EMT) markers, and (D) cancer stem cell (CSC) markers in PVA-treated PK-8, MIA PaCa-2 cells, or their control cells using qRT-PCR. Flow cytometry analyses of (B) β1 and α2 integrin and (F) CD24 and CD44v9 in PK-8 cells. (E) Western blot analysis of Nanog and Sox2 in PK-8 cells. Results are presented as the mean ± SD of four or three independent experiments for qRT-PCR. Western blot analysis was independently performed twice and representative densitometric data of the protein normalized to β-actin is shown. See full images in Supplementary Figure 1. Mean fluorescence intensities (MFIs) relative to those in control cells based on three independent experiments are shown at lower panels in (B) and (F). *$p < 0.05$, **$p < 0.01$.
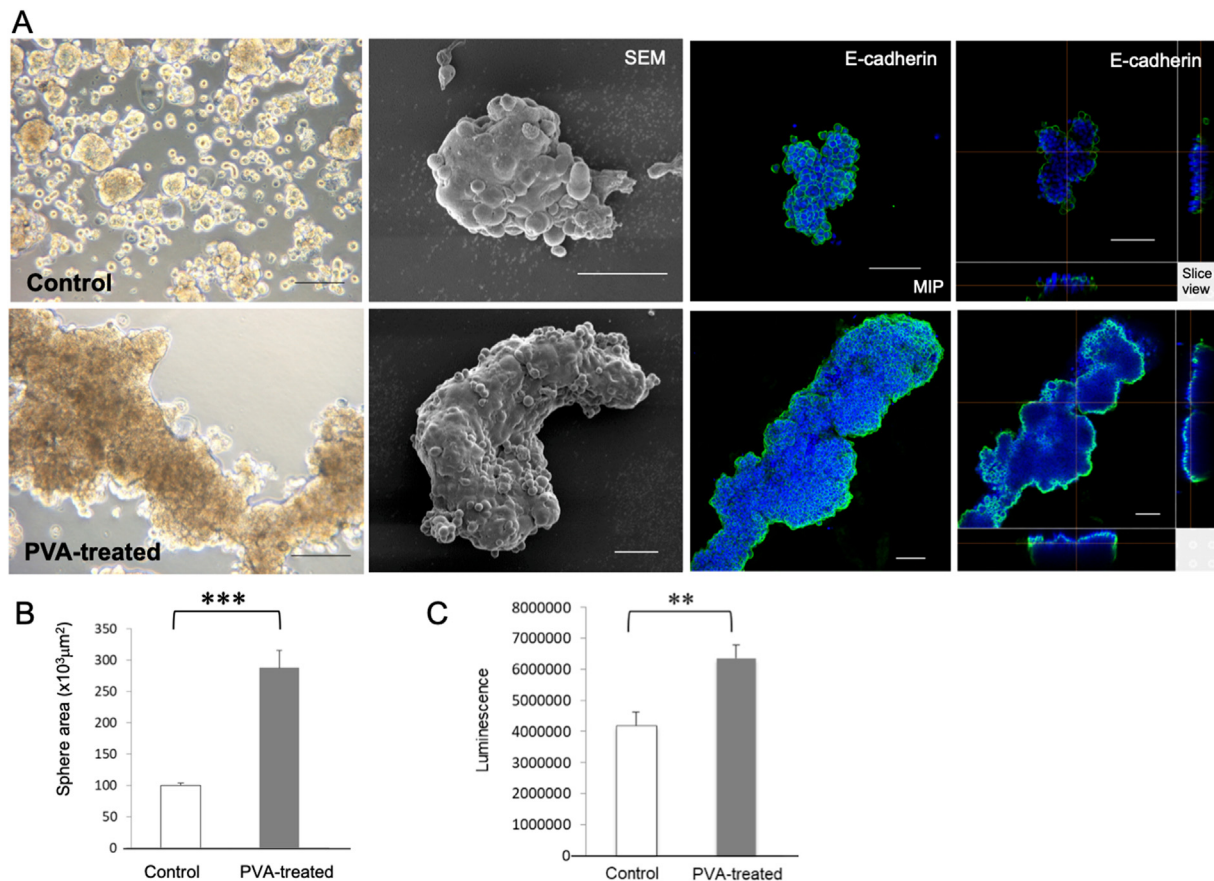

Figure 3. Effects of PVA on the morphology, cell growth, and E-cadherin expression of PVA-treated PK-8 cells under 3D-culture conditions. (A) PVA-treatment induced rod-like appearance in PK-8 cells. E-cadherin was expressed in the cell membranes of the PK-8 cells, especially at the periphery of the spheres. Green: E-cadherin, Blue: Nucleus. Scale bar in the phase contrast, maximum intensity projection (MIP), and slice view images: 100 μm. Scale bar in the SEM images: 50 μm. PVA induced larger sphere sizes (B) and higher cell growth of the PK-8 cells (C). **$p < 0.01$, ***$p < 0.001$.

needed, but the increase in α2β1 integrin mediated adhesion to matrix may be one of the mechanisms of promotion of invasive capacity after the addition of PVA. A previous study has shown that PVA caused marked expansion of functional multipotent self-renewing hematopoietic stem cells [10]. In the 2D-culture of PK-8 cells, 4 out of 7 major pancreatic CSC markers were significantly increased, while only *Nestin* was decreased. This suggests that, following the addition of PVA, aggregated colonies of PK-8 cells contain more CSCs, and that PVA increases the CSC population under 2D-culture conditions with serum-free medium.

Recently, 3D-cultures of cancer cells have garnered attention because they morphologically and functionally mimic cancer cells *in vivo* [5]. In the sphere-formation assay, when PDACs are cultured in ultra-low attachment dishes, the PDAC cells form floating colonies with prominent CSCs [22]. In a previous study using a sphere-formation assay, we reported that extracellular stimuli and different cell culture conditions induced functional and morphological heterogeneity in PDAC cells [8]. In this study, PK-8 cells formed round to oval-shaped spheres, while the addition of PVA induced the formation of larger spheres with a rod-like appearance. It is considered that this morphological alteration of the spheres is the result of the spheres fusing with each other using cell

attachment molecules, including E-cadherin, and increased proliferation among the PK-8 cells in the PVA-treated group. Interestingly, none of the CSC markers were significantly increased in the spheres of the PVA-treated group, nor were any of the drug transporters that we examined. This suggests that the addition of PVA enlarged the spheres with a higher population of non-CSCs.

Recent studies, including ours, have shown that PDACs are heterogeneous tumors [6, 23]. PVA treatment resulted in different morphological alterations in the three pancreatic cancer cell lines. Moreover, gene expression patterns were different in PK-8 and MIA PaCa-2 cells, although these two types of cell lines formed similar mountain-like colonies in the 2D-culture. This suggests that the effects of PVA may differ for each pancreatic cancer cell type.

In summary, PVA increased PK-8 cell proliferation, migration, invasion, and CSC marker expression in the 2D-culture under serum-free conditions. In 3D-culture, PVA induced PK-8 cell proliferation and formation of larger spheres, but did not increase CSC marker expression. These findings suggest that PVA affects the behavior of PK-8 cells, but does not contribute to the increase in CSCs in serum-free 3D-culture.
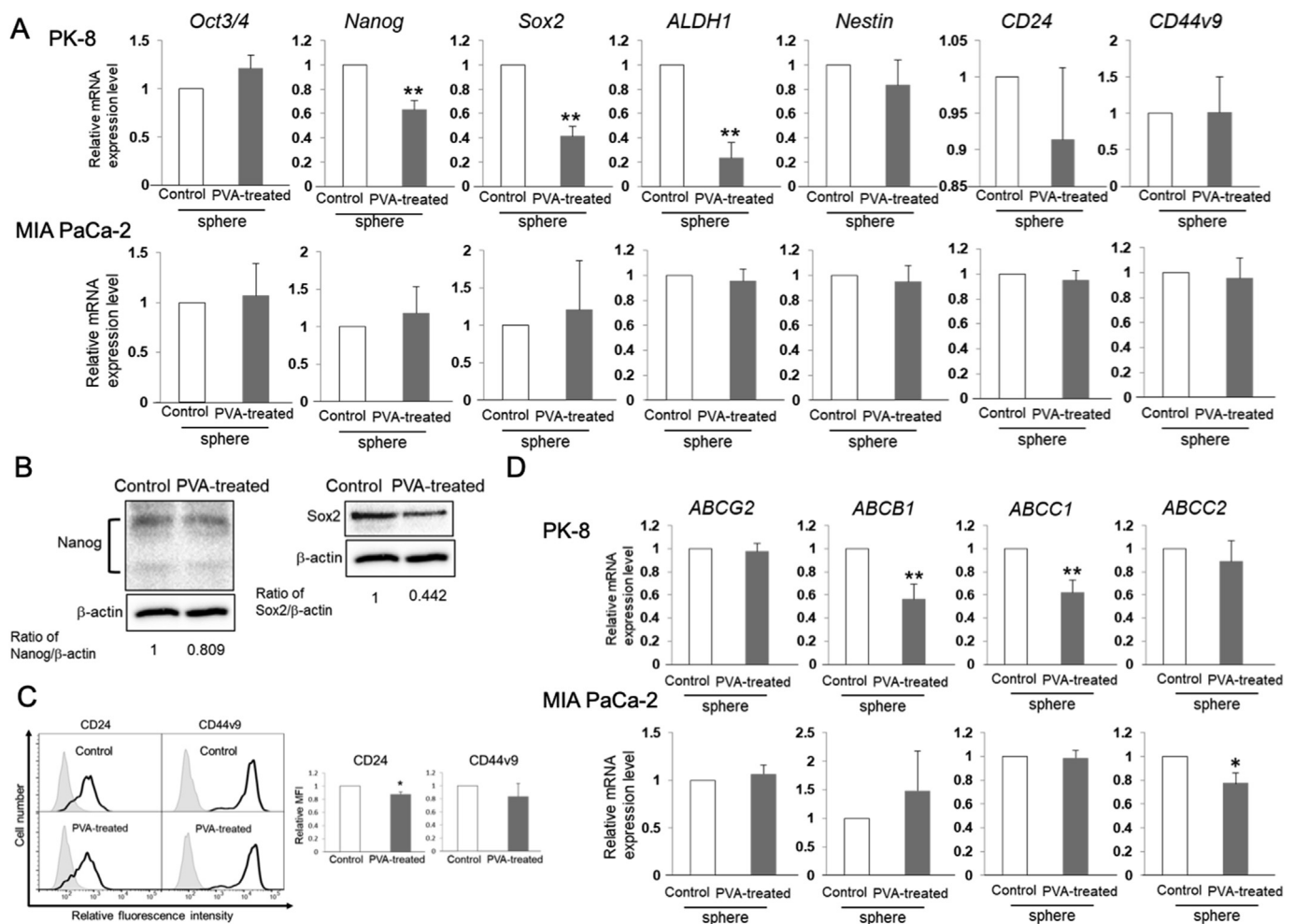
Figure 4. Expression of CSC markers and drug transporters in the PVA-treated cells under 3D-culture conditions. Comparative expression of (A) CSC markers and (D) drug transporters by PVA-treated PK-8 and MIA PaCa-2 cells and their control cells using qRT-PCR. (B) Western blot analysis of Nanog and Sox2 in PK-8 cells. See full images in Supplementary Figure 2. (C) Flow cytometry analysis of CD24 and CD44v9 in PK-8 cells. Results are presented as the mean $\pm$ SD of four or three independent experiments for qRT-PCR. $**p < 0.01$. Western blot analysis was performed twice independently, and representative densitometric data normalized to β-actin is shown. Mean fluorescence intensities (MFIs) relative to those in control cells based on three independent experiments are shown in the right panels in (C).

Declarations

Author contribution statement

Fujiya Gomi, Norihiko Sasaki, Toshiyuki Ishiwata: Conceived and designed the experiments; Wrote the paper.

Yuuki Shichi, Fuuka Minami, Seiichi Shinji: Performed the experiments; Analyzed and interpreted the data.

Masashi Toyoda: Analyzed and interpreted the data.

Funding statement

Data availability statement

Data included in article/supplementary material/referenced in article.

Declaration of interests statement

The authors declare no conflict of interest.

Additional information

Supplementary content related to this article has been published online at https://doi.org/10.1016/j.heliyon.2021.e06182.

Acknowledgements

References

[1] R.L. Siegel, K.D. Miller, A. Jemal, Cancer statistics, 2020, CA Cancer J. Clin. 70 (2020) 7–30.
[2] A. Jemal, R. Siegel, E. Ward, Y. Hao, J. Xu, T. Murray, M.J. Thun, Cancer statistics, 2008, CA A Cancer J. Clin. 58 (2008) 71–96.

[3] L. Rahib, B.D. Smith, R. Aizenberg, A.B. Rosenzweig, J.M. Fleshman, L.M. Matrisian, Projecting cancer incidence and deaths to 2030: the unexpected burden of thyroid, liver, and pancreas cancers in the United States, Canc. Res. 74 (2014) 2913–2921.

[4] T. Ishiwata, Cancer stem cells and epithelial-mesenchymal transition: novel therapeutic targets for cancer, Pathol. Int. 66 (2016) 601–608.

[5] T. Ishiwata, Y. Matsuda, H. Yoshimura, N. Sasaki, S. Ishiwata, N. Ishikawa, K. Takubo, T. Arai, J. Aida, Pancreatic cancer stem cells: features and detection methods, Pathol. Oncol. Res. 24 (2018) 797–805.

[6] Y. Shichi, N. Sasaki, M. Michishita, F. Hasegawa, Y. Matsuda, T. Arai, F. Gomi, J. Aida, K. Takubo, M. Toyoda, H. Yoshimura, K. Takahashi, T. Ishiwata, Enhanced morphological and functional differences of pancreatic cancer with epithelial or mesenchymal characteristics in 3D culture, Sci. Rep. 9 (2019) 10871.

[7] M.F. Clarke, J.E. Dick, P.B. Dirks, C.J. Eaves, C.H. Jamieson, D.L. Jones, J. Visvader, I.L. Weissman, G.M. Wahl, Cancer stem cells–perspectives on current status and future directions: AACR Workshop on cancer stem cells, Canc. Res. 66 (2006) 9339–9344.

[8] N. Sasaki, M. Toyoda, F. Hasegawa, M. Fujiwara, F. Gomi, T. Ishiwata, Fetal bovine serum enlarges the size of human pancreatic cancer spheres accompanied by an increase in the expression of cancer stem cell markers, Biochem. Biophys. Res. Commun. 514 (2019) 112–117.

[9] M.I. Baker, S.P. Walsh, Z. Schwartz, B.D. Boyan, A review of polyvinyl alcohol and its uses in cartilage and orthopedic applications, J. Biomed. Mater. Res. B Appl. Biomater. 100 (2012) 1451–1457.

[10] A.C. Wilkinson, R. Ishida, M. Kikuchi, K. Sudo, M. Morita, R.V. Crisostomo, R. Yamamoto, K.M. Loh, Y. Nakamura, M. Watanabe, H. Nakauchi, S. Yamazaki, Author Correction: long-term ex vivo haematopoietic-stem-cell expansion allows nonconditioned transplantation, Nature 571 (2019) E12.

[11] N. Sasaki, K. Hirabayashi, M. Michishita, K. Takahashi, F. Hasegawa, F. Gomi, Y. Itakura, N. Nakamura, M. Toyoda, T. Ishiwata, G.M.2 Ganglioside, Highly expressed in the MIA PaCa-2 pancreatic ductal adenocarcinoma cell line, is correlated with growth, invasion, and advanced stage, Sci. Rep. 9 (2019) 19369.

[12] N. Sasaki, T. Ishiwata, F. Hasegawa, M. Michishita, H. Kawai, Y. Matsuda, T. Arai, N. Ishikawa, J. Aida, K. Takubo, M. Toyoda, Stemness and anti-cancer drug resistance in ATP-binding cassette subfamily G member 2 highly expressed pancreatic cancer is induced in 3D culture conditions, Canc. Sci. 109 (2018) 1135–1146.

[13] N. Sasaki, M. Toyoda, H. Yoshimura, Y. Matsuda, T. Arai, K. Takubo, J. Aida, T. Ishiwata, H19 long non-coding RNA contributes to sphere formation and invasion through regulation of CD24 and integrin expression in pancreatic cancer cells, Oncotarget 9 (2018) 34719–34734.

[14] C.C. DeMerlis, D.R. Schoneker, Review of the oral toxicity of polyvinyl alcohol (PVA), Food Chem. Toxicol. 41 (2003) 319–326.

[15] S.R. Van Tomme, G. Storm, W.E. Hennink, In situ gelling hydrogels for pharmaceutical and biomedical applications, Int. J. Pharm. 355 (2008) 1–18.

[16] T. Nomoto, Y. Inoue, Y. Yao, M. Suzuki, K. Kanamori, H. Takemoto, M. Matsui, K. Tomoda, N. Nishiyama, Poly(vinyl alcohol) boosting therapeutic potential of p-boronophenylalanine in neutron capture therapy by modulating metabolism, Sci. Adv. 6 (2020) eaaz1722.

[17] C. Ricci, C. Mota, S. Moscato, D. D'Alessandro, S. Ugel, S. Sartoris, V. Bronte, U. Boggi, D. Campani, N. Funel, L. Moroni, S. Danti, Interfacing polymeric scaffolds with primary pancreatic ductal adenocarcinoma cells to develop 3D cancer models, Biomatter 4 (2014), e955386.

[18] V. Yagublu, N. Caliskan, A.L. Lewis, R. Jesenofsky, L. Gasimova, J.M. Lohr, M. Keese, Treatment of experimental pancreatic cancer by doxorubicin-, mitoxantrone-, and irinotecan-drug eluting beads, Pancreatology 13 (2013) 79–87.

[19] R.E. Forster, S.A. Small, Y. Tang, C.L. Heaysman, A.W. Lloyd, W. Macfarlane, G.J. Phillips, M.D. Antonijevic, A.L. Lewis, Comparison of DC Bead-irinotecan and DC Bead-topotecan drug eluting beads for use in locoregional drug delivery to treat pancreatic cancer, J. Mater. Sci. Mater. Med. 21 (2010) 2683–2690.

[20] E.J. Slapak, J. Duitman, C. Tekin, M.F. Bijlsma, C.A. Spek, Matrix metalloproteases in pancreatic ductal adenocarcinoma: key drivers of disease progression? Biology (Basel) 9 (2020).

[21] M. Bloomston, E.E. Zervos, A.S. Rosemurgy 2nd, Matrix metalloproteinases and their role in pancreatic cancer: a review of preclinical studies and clinical trials, Ann. Surg Oncol. 9 (2002) 668–674.

[22] T. Ishiwata, F. Hasegawa, M. Michishita, N. Sasaki, N. Ishikawa, K. Takubo, Y. Matsuda, T. Arai, J. Aida, Electron microscopic analysis of different cell types in human pancreatic cancer spheres, Oncol. Lett. 15 (2018) 2485–2490.

[23] E.A. Collisson, A. Sadanandam, P. Olson, W.J. Gibb, M. Truitt, S. Gu, J. Cooc, Subtypes of pancreatic ductal adenocarcinoma and their differing responses to therapy, Nat. Med. 17 (2011) 500–503.